ELSEVIER

Journal of Alloys and Compounds 217 (1995) 287–294

Journal of ALLOYS AND COMPOUNDS

Reactive mechanical grinding of ZrNi under various partial pressures of hydrogen

S. Orimo [1], H. Fujii *, T. Yoshino

Faculty of Integrated Arts and Sciences, Hiroshima University, Higashi-Hiroshima, 724, Japan

Received 26 May 1994, in final form 26 July 1994

Abstract

The intermetallic compound ZrNi was mechanically ground under various partial pressures of hydrogen. At the beginning of the grinding, hydride phases (ZrNiH and/or $ZrNiH_3$) are formed, which lowers the free energy of the compound, and the particle size are effectively reduced. Moreover, with progression of the grinding, an amorphous phase starts to grow. Finally, depending on the partial pressure of hydrogen, a composite particle of the amorphous and crystalline phases is formed. Consequently, such a grinding technique under various partial pressures of hydrogen promotes the synthesis of fine composite particles, each of which consists of amorphous hydride and the crystalline hydride phases. In addition, the grinding enhances the decomposition to form ZrH_2 even at room temperature. During the heating process under an argon atmosphere, the dehydrogenation of ZrH_2 can progress even at low temperatures of around 750 K, which is caused by preferential crystallization of the amorphous phases in the fine composite particles.

Keywords: Reactive mechanical grinding; Composite particle; Amorphous hydride phase; Crystalline hydride phase; Preferential crystallization

1. Introduction

Mechanical grinding (MG) is an attractive method for synthesizing amorphous materials in the solid state [1–5]. Generally in this method, particles of intermetallic compounds are ground under an inert gas atmosphere. Recently, mechanical grinding or alloying processes accompanied by solid–gas reactions under active gas atmospheres such as hydrogen, nitrogen and oxygen have been intensively investigated [6–10].

In this work, we tried to grind the intermetallic compound ZrNi under various partial pressures of hydrogen. The motivation was that two effects are considered to be added to the usual mechanical grinding as a result of the hydriding reaction during the grinding, as illustrated in Fig. 1 and outlined below.

One of the two effects is a lowering of the free energy of the compound against the inherent property of mechanical grinding, which only raises it by the external mechanical energy. The compound, which is going to be transformed into the metastable state, forms hydrides to lower the free energy under hydrogen-containing atmospheres. In some cases, the hydriding reaction leads to decomposition to form elemental hydrides. From the viewpoint of free energy, the reactive mechanical grinding involves a competition regarding the transforming directions, lowering or raising the free energy of the compound. Therefore, it is expected that

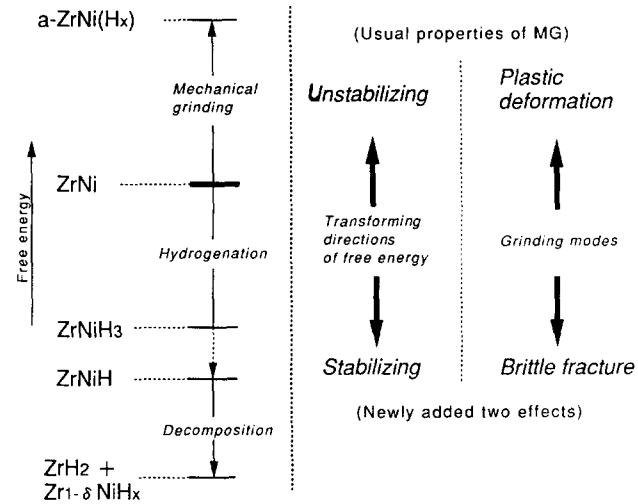

Fig. 1. Two effects added to the usual mechanical grinding as a result of hydriding reaction: lowering of the free energy of the compounds and addition of brittle fracture mode.

* Corresponding author.

[1] Research Fellow of the Japan Society for the Promotion of Science.

SSDI 0925-8388(94)01354-3

composite particles of amorphous and crystalline phases can be synthesized.

The other effect is the brittle fracture mode. This mode is against the normal mechanical grinding which acts plastically to the external mechanical energy. Our preliminary experiments confirmed that ZrNi does not easily change its particle size during the usual grinding and it does not react with an atmosphere at all. In contrast, hydrides of ZrNi are so brittle that external mechanical energy was consumed for the reduction of their particle sizes. Consequently, we consider that fine particles of the composite phase can be effectively synthesized by reactive mechanical grinding as described in this paper.

To confirm the additional effects described above, particle morphology, hydrogenation and amorphization properties of ZrNi during reactive mechanical grinding were investigated under various partial pressures of hydrogen. Furthermore, the crystallization and dehydrogenation properties of the synthesized particles were examined by thermogravimetric/differential thermal analysis (TG/DTA).

2. Experimental

The initial compound ZrNi was prepared by arc melting of each element of 99.9% purity under an argon atmosphere. Bulk ZrNi is ductile and the surfaces of its powder are active for oxygen and nitrogen. Therefore, it was pre-treated with hydrogen to reduce the grain size whilst maintaining the surface activity under the following conditions. After degassing for 12 h, ZrNi was heated to 573 K. Three repetitive hydriding under a hydrogen pressure of 1 MPa (99.99999% purity) and dehydriding under vacuum were performed on ZrNi, and finally dehydriding at 673 °K to remove the hydrogen completely from it. As a result of this pre-treatment, the bulk property of ZrNi changed to sufficiently brittle to be effectively ground.

Both the pre-treated bulk ZrNi (1 g) and 20 steel balls of 7 mm diameter (weight ratio nearly 1:30) were placed in a steel vial of 30 cm^3 volume. The vial, which was equipped with a connection valve for vacuuming or introduction of various gases, was degassed for 12 h below 1.0 Pa. Then, mixed high-purity hydrogen and argon were introduced into it, the pressures of which were up to 1.0 MPa. The mixing ratios of these gases were 0:10, 1:9, 3:7 and 10:0, which correspond to partial hydrogen pressures of 0, 0.1, 0.3 and 1.0 MPa, respectively. They were ground at a rotation speed of nearly 400 rpm for periods from 5 min to 80 h (Fritsch P7). For grinding longer than 3 h, cycles with rotation for 3 h and pausing for 1 h were repeated to minimize sample heating.

The particles thus synthesized under various partial pressures of hydrogen and grinding times were characterized by X-ray diffraction (Mac Science MXP3, Cu Kα radiation), scanning electron microscopy (Hitachi S-4100), and TG/DTA (Seiko TG/DTA300). The thermal analyses were carried out under a pure argon atmosphere with heating at 5 K min^{-1} to 873 K.

3. Results

3.1. Phases of initial compound before and after pre-treatment

Fig. 2 shows the X-ray diffraction profiles for ZrNi before and after the pre-treatment of three hydriding and dehydriding cycles as mentioned above. The results confirmed that the phase is not changed at all by the pre-treatment.

3.2. Phase transformations of particles during the reactive mechanical grinding

X-ray diffraction profiles for the particles ground under a pure argon pressure of 1.0 MPa (a partial hydrogen pressure of 0 MPa) are shown in Fig. 3. After 5 min from the beginning of the grinding, the phase has not changed despite a slight broadening of the peaks. After 5 h the crystalline peaks disappear, and finally after grinding for 80 h the single phase of amorphous ZrNi (a-ZrNi) is formed.

Fig. 4 shows the X-ray diffraction profiles for the particles ground under a partial hydrogen pressure of 0.1 MPa. The profile of the particles ground for 5 min shows not only a broadening but also a shift of some

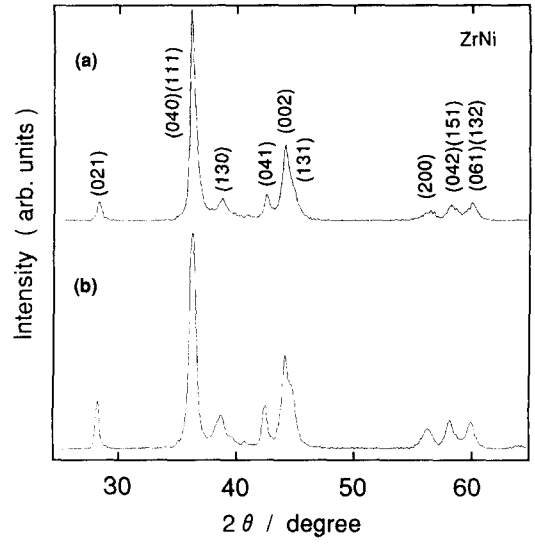

Fig. 2. X-ray diffraction profiles (Cu Kα) for the initial compound, (a) before and (b) after pre-treatment with three hydriding and dehydriding cycles.

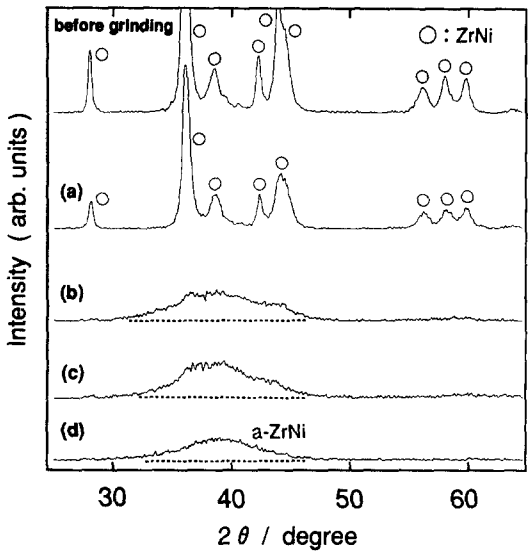

Fig. 3. X-ray diffraction profiles (Cu Kα) for the particles ground under a pure argon pressure of 1.0 MPa (a partial hydrogen pressure of 0 MPa) for (a) 5 min, (b) 5 h, (c) 20 h and (d) 80 h. To clarify the existence of an amorphous phase, broken lines are shown as a background in some profiles.

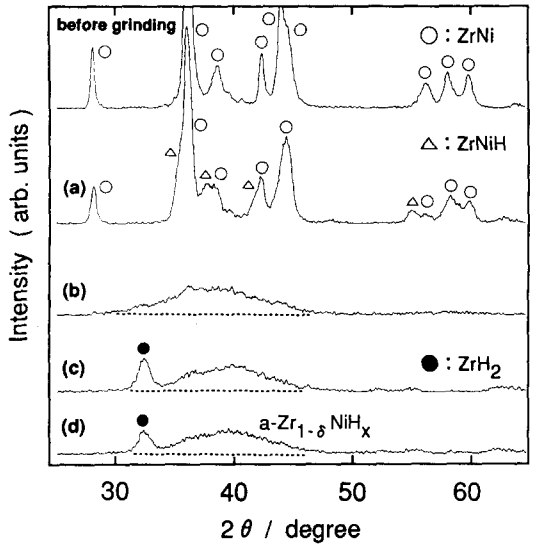

Fig. 4. X-ray diffraction profiles (Cu Kα) for the particles ground under a partial hydrogen pressure of 0.1 MPa for (a) 5 min, (b) 5 h, (c) 20 h and (d) 80 h.

peaks to lower angles. This shift is probably caused by the formation of ZrNiH [11]. After 5 h, the profile is almost the same as in Fig. 3(b), in which crystalline peaks have disappeared. For grinding times longer than 20 h, however, the decomposition product ZrH_2 and the amorphous hydride a-$Zr_{1-\delta}NiH_x$ are newly formed (here $Zr_{1-\delta}Ni$ means that the atomic ratio of elemental Zr is less than that of Ni, owing to the consumption of some amount of elemental Zr to form ZrH_2). It is noted that the intensity of the peaks corresponding to ZrH_2 is decreased in the profile at 80 h (Fig. 4(d)) compared with that at 20 h.

To clarify the phase transformations in the first stage of the grinding under a partial hydrogen pressure of 0.3 MPa, the phases with shorter periods of grinding were examined by X-ray diffraction, the results of which are shown in Fig. 5. After 5 min from the beginning of the grinding, both ZrNiH and $ZrNiH_3$ are formed. On further grinding, all the peaks broaden whilst keeping the same relative intensity ratios. After 5 h, a-$Zr_{1-\delta}NiH_x$ is formed and ZrH_2 starts to be detected. The peak intensity of ZrH_2 decreases with grinding times longer than 20 h, as observed in that under 0.1 MPa of hydrogen.

Finally, X-ray diffraction profiles for the particles ground under a pure hydrogen pressure of 1.0 MPa are shown in Fig. 6. A single phase of $ZrNiH_3$ is formed within 5 min, but the phases change little after that. After 20 h, both ZrH_2 and a-$Zr_{1-\delta}NiH_x$ start to be detected in addition to $ZrNiH_3$.

3.3. Morphology transformations of particles during the reactive mechanical grinding

Fig. 7 shows SEM images for the particles ground under a pure argon atmosphere (the left-hand images are at a magnification of ×500 and the right-hand images at a higher magnification of ×3000). The particle sizes are gradually reduced to around 50 μm in diameter after grinding for 5 h, and little change can be observed with grinding times longer than 20 h. After 80 h, a-ZrNi particles 20–50 μm in diameter only can be obtained as host particles, and no decomposed particles at the surface of the host can be observed even with higher magnification.

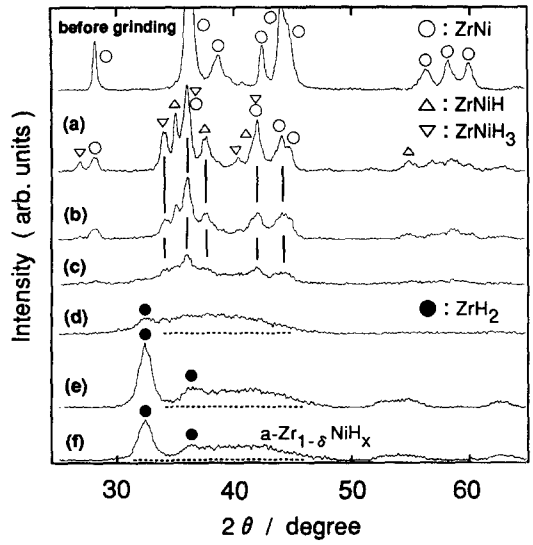

Fig. 5. X-ray diffraction profiles (Cu Kα) for the particles ground under a partial hydrogen pressure of 0.3 MPa for (a) 5 min, (b) 15 min, (c) 1 h, (d) 5 h, (e) 20 h and (f) 80 h.

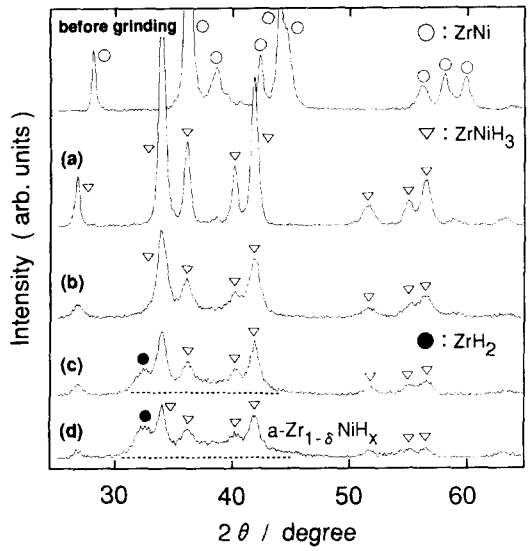

Fig. 6. X-ray diffraction profiles (Cu Kα) for the particles ground under a pure hydrogen pressure of 1.0 MPa for (a) 5 min, (b) 5 h, (c) 20 h and (d) 80 h.

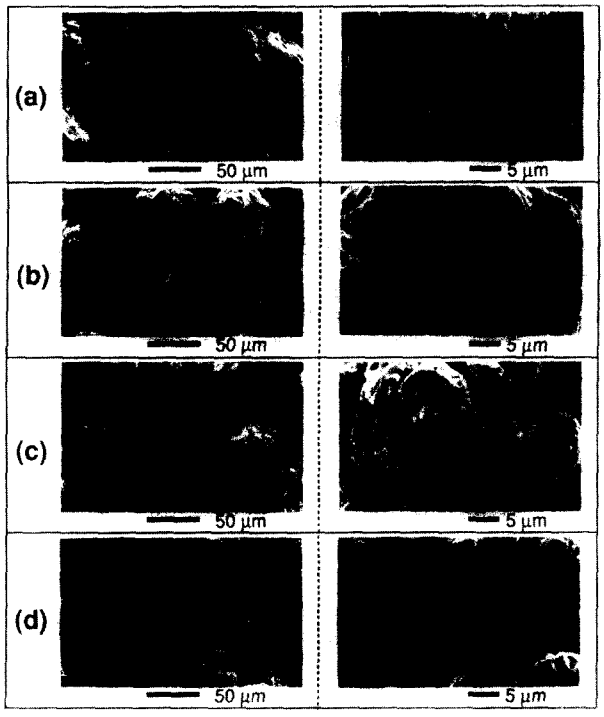

Fig. 7. SEM images for the particles ground under a pure argon pressure of 1.0 MPa (a partial hydrogen pressure of 0 MPa) for (a) 5 min, (b) 5 h, (c) 20 h and (d) 80 h.

SEM images for the particles ground under a partial hydrogen pressure of 0.1 MPa are shown in Fig. 8. After 5 min, we can observe not only fine decomposed particles about 1 μm in diameter, which seems to correspond to ZrNiH, but also some fracture cracks in the host particles. The sizes of the host particles are slightly finer (about 20 μm) than those under a pure argon atmosphere, but little difference can be observed with grinding times longer than 20 h (20–50 μm). Since fine decomposed particles cannot be observed in the images after longer grinding times (Fig. 8(d)), they seem to penetrate into the host particles with progression of the grinding.

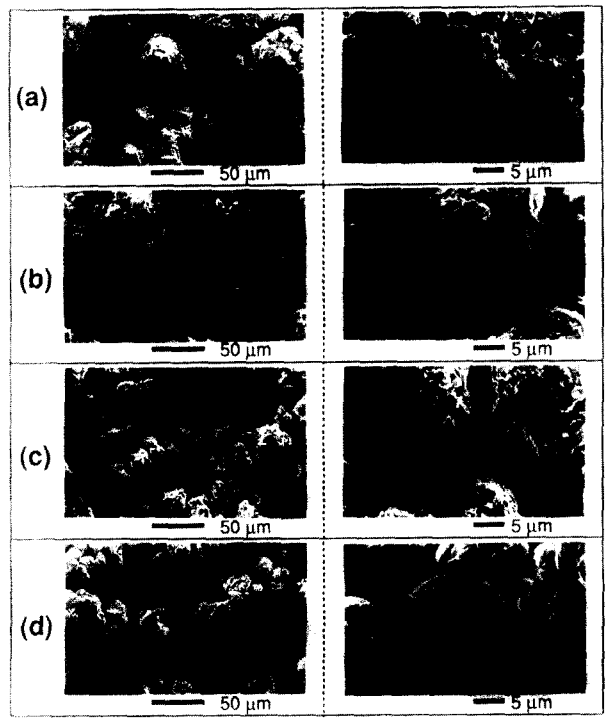

Fig. 8. SEM images for the particles ground under a partial hydrogen pressure of 0.1 MPa for (a) 5 min, (b) 5 h, (c) 20 h and (d) 80 h.

There are obvious morphological differences between the particles ground under a partial hydrogen pressure of 0.1 MPa and those under higher (partial) pressures, which are shown in Figs. 9 and 10. In Fig. 9, the amounts of fine decomposed particles are much larger than those under 0.1 MPa of hydrogen, and disintegration of the host particles progresses even within 5 min. These host particles of diameter less than 10 μm, to which adhere the fine decomposed particles, correspond to ZrNiH or $ZrNiH_3$. After 5 h, fine decomposed particles seem to penetrate into the host particles with a smooth surface, and the whole particles become coarser. Judging from Fig. 5(d), the host particles in the images after 5 h of grinding correspond to a-$Zr_{1-\delta}NiH_x$. The particle sizes are reduced again after 20 h, but they do not change any more with further grinding (about 5 μm). Under 1.0 MPa of pure hydrogen, as shown in Fig. 10, there is further formation of decomposed particles and disintegration of host particles. We can observe that the particles ground for 5 h are finest (0.5–1 μm), and they gradually become coarser with further grinding.

3.4. Crystallization and dehydrogenation properties of synthesized particles

The particles ground for 80 h under various partial pressures of hydrogen were heated under a pure argon

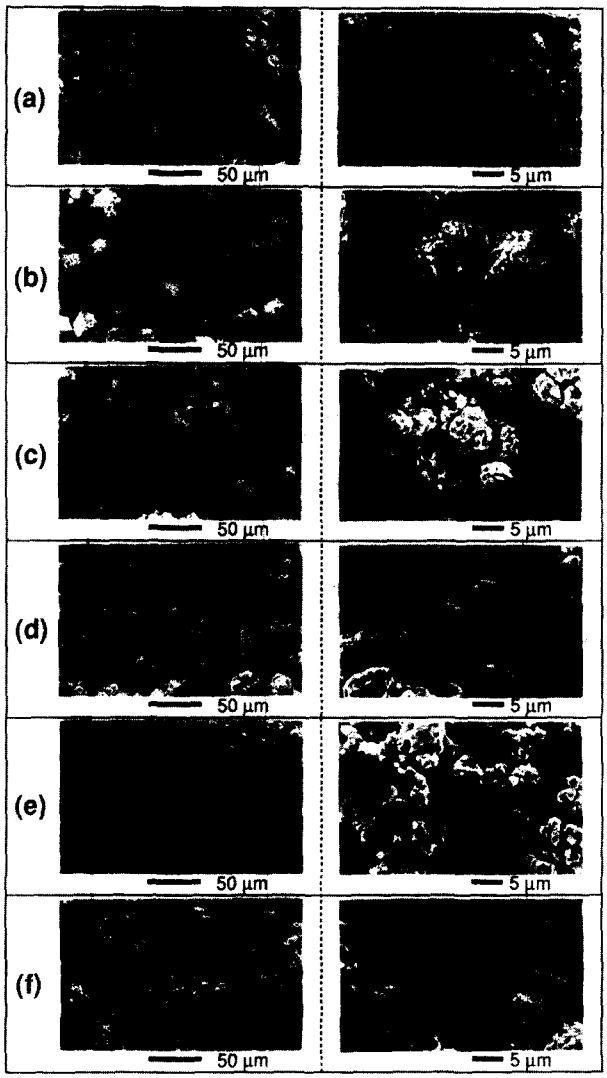

Fig. 9. SEM images for the particles ground under a partial hydrogen pressure of 0.3 MPa for (a) 5 min, (b) 15 min, (c) 1 h, (d) 5 h, (e) 20 h and (f) 80 h.

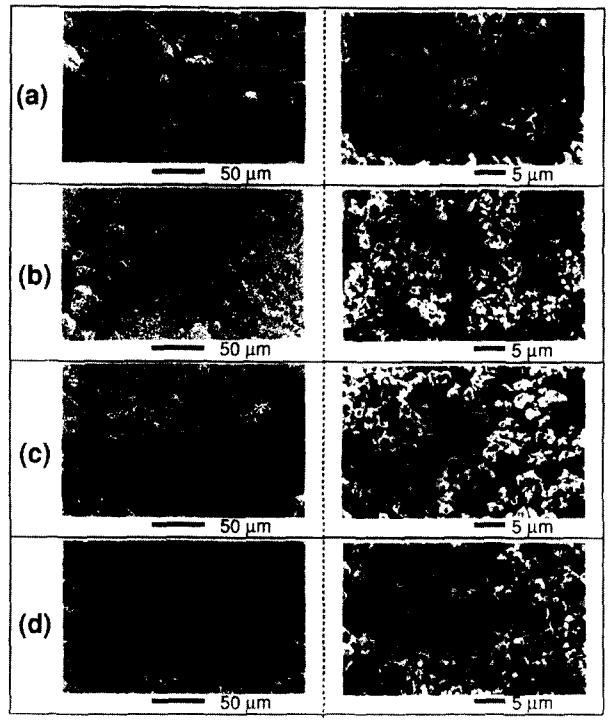

Fig. 10. SEM images for the particles ground under a pure hydrogen pressure of 1.0 MPa for (a) 5 min, (b) 5 h, (c) 20 h and (d) 80 h.

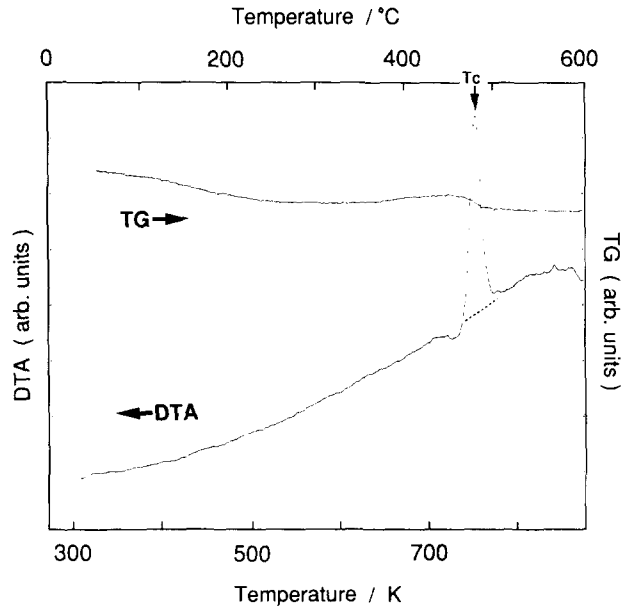

Fig. 11. TG/DTA profiles for the particles ground under a pure argon pressure of 1.0 MPa (a partial hydrogen pressure of 0 MPa) for 80 h. To clarify the deviation from the background of each temperature, broken lines are shown here and in subsequent profiles.

atmosphere, and their crystallization and dehydrogenation (hydrogen dissociation from amorphous phase) properties were examined.

Fig.11 shows the TG/DTA profiles for the particles ground under a pure argon atmosphere. The TG profile does not change at all because the particles did not react with the atmosphere during the grinding. An exothermic peak (T_c=749 K) in the DTA profile corresponds to the crystallization of a-ZrNi.

The particles ground under 0.1 MPa of hydrogen start to reduce their weights at around 630 K, as shown in Fig. 12. Judging from experimental and theoretical data in previous reports [12–15], this reduction corresponds to the dissociation of hydrogen atoms which were trapped by the 3Zr1Ni sites (the sites surrounded by three elemental Zr and one elemental Ni) in a-$Zr_{1-\delta}NiH_x$. At higher temperatures, we can also detect crystallization (T_c=747 K) and hydrogen dissociation from 4Zr sites in a-$Zr_{1-\delta}NiH_x$. An endothermic peak (T_d=791 K) corresponds to the dehydrogenation of ZrH_2.

Similarly, the particles ground under 0.3 MPa of hydrogen show gradual hydrogen dissociation from a-$Zr_{1-\delta}NiH_x$ above 420 K, as shown in Fig. 13. Thus, hydrogen atoms were trapped in 2Zr2Ni sites in addition to both the 4Zr and 3Zr1Ni sites. Sequential reactions

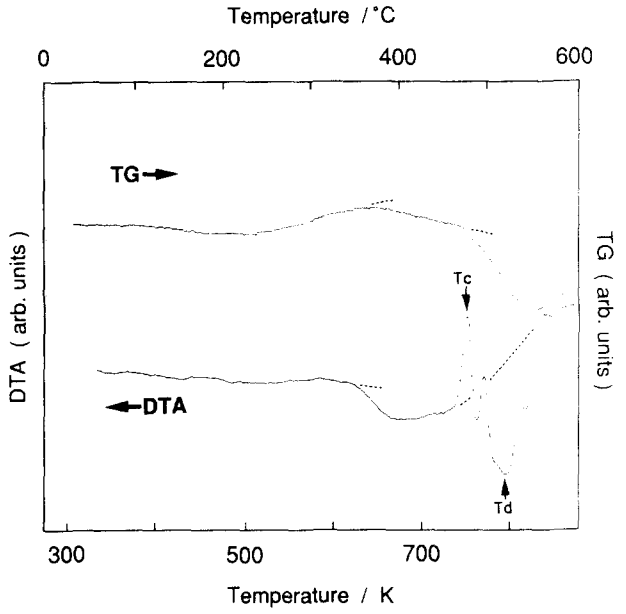

Fig. 12. TG/DTA profiles for the particles ground under a partial hydrogen pressure of 0.1 MPa for 80 h.

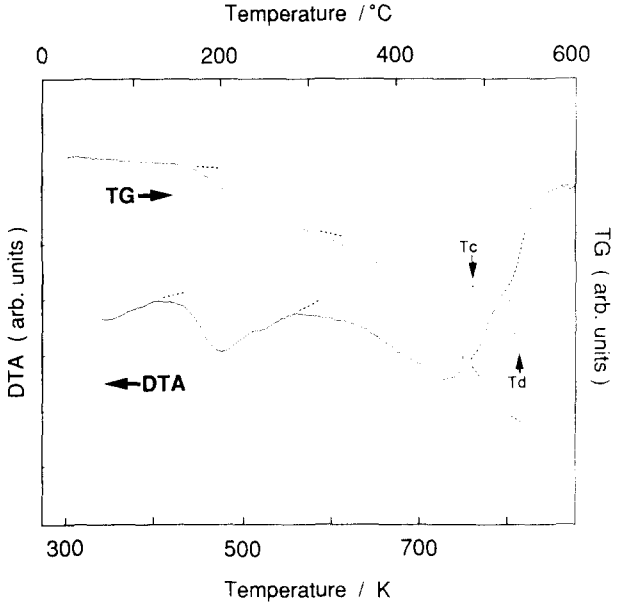

Fig. 13. TG/DTA profiles for the particles ground under a partial hydrogen pressure of 0.3 MPa for 80 h.

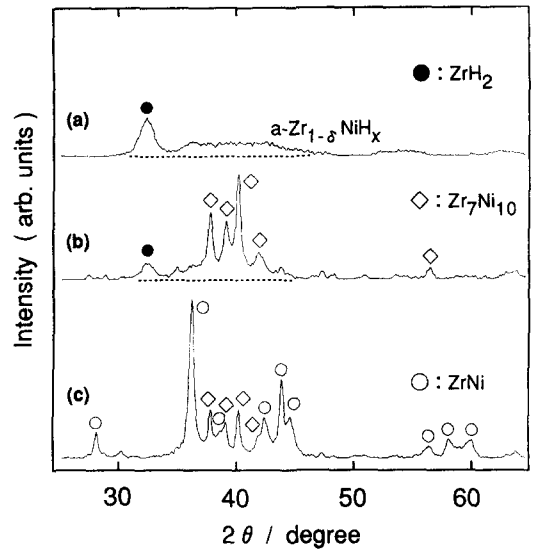

Fig. 14. X-ray diffraction profiles (Cu Kα) for the particles ground under a partial hydrogen pressure of 0.3 MPa, (a) before the heat treatment, and after heat treatment at (b) 773 K and (c) 853 K.

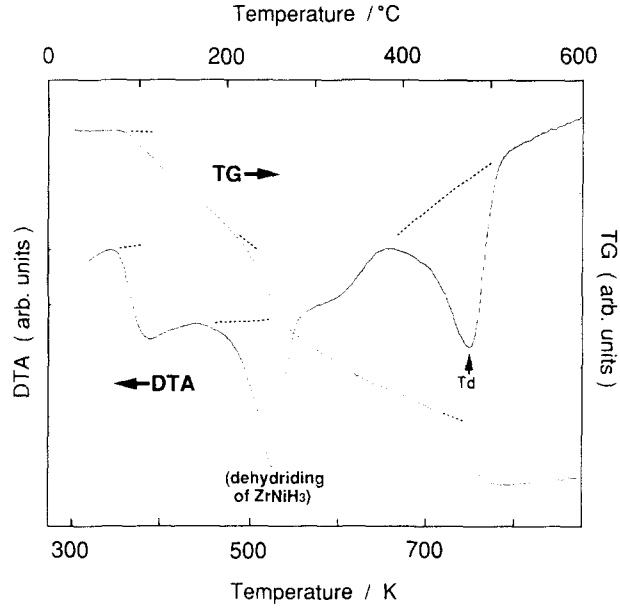

Fig. 15. TG/DTA profiles for the particles ground under a pure hydrogen pressure of 1.0 MPa for 80 h.

of crystallization followed by hydrogen dissociation are detected more clearly than those in the profiles in Fig. 12. Fig. 14 shows the X-ray diffraction profiles for the particles heat-treated just below and above the temperatures of an endothermic peak (T_d=810 K) which corresponds to the dehydrogenation of ZrH_2 in Fig. 13. These profiles indicate that ZrNi in Fig. 14(c) is formed by the solid–solid reaction between the ZrH_2 phase formed during the grinding and Zr_7Ni_{10} phase formed by crystallization (T_c=757 K) during the heating process after the grinding. At the same time as progression of this solid–solid reaction, hydrogen atoms dissociate from ZrH_2. These sequential reactions are the same as observed in a previous investigation [16].

Finally, the TG/DTA profiles for the particles ground under 1.0 MPa of pure hydrogen are shown in Fig. 15. Since a weight reduction already starts below 373 K, it is deduced that hydrogen atoms were trapped even by unstable sites of 2Zr2Ni. The X-ray diffraction analyses confirmed that an endothermic peak at 525 K corresponds to the dehydrogenation of $ZrNiH_3$.

Although the results of TG/DTA analyses at lower temperatures as described above can be easily understood, the results obtained at higher temperatures imply peculiar properties of the composite particles. One is

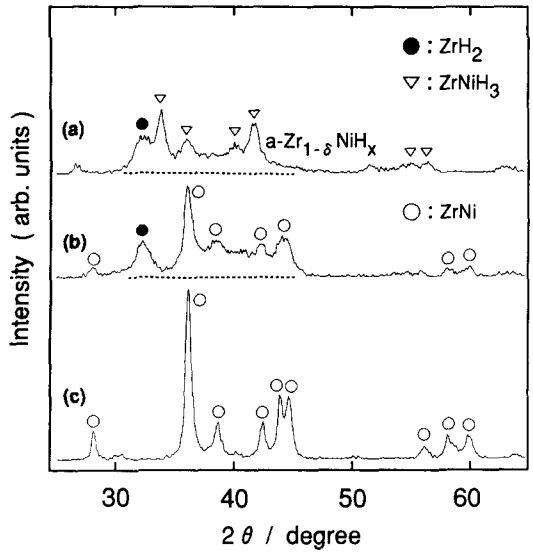

Fig. 16. X-ray diffraction profiles (Cu Kα) for the particles ground under a pure hydrogen pressure of 1.0 MPa, (a) before the heat treatment, and after heat treatment at (b) 693 K and (c) 783 K.

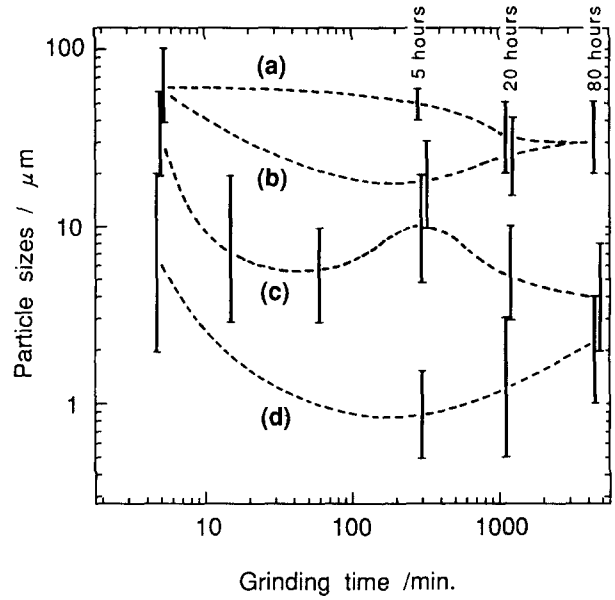

Fig. 17. Size changes of the particles ground under (partial) hydrogen pressures of (a) 0, (b) 0.1, (c) 0.3 and (d) 1.0 MPa.

that no exothermic peak of DTA analysis corresponding to crystallization of a-$Zr_{1-\delta}NiH_x$ is detected in Fig. 15. Regarding the particles ground under hydrogen pressures lower than 0.3 MPa, such peaks are obviously detected around 750 K. Another is that the dehydriding temperature of ZrH_2 ($T_d = 746$ K) is lower by as much as 64 K than that under 0.3 MPa of hydrogen, and it comes close to the crystallization temperature of a-$Zr_{1-\delta}NiH_x$. X-ray diffraction profiles for the particles heat-treated just below and above the temperatures of the endothermic peak ($T_d = 746$ K) which mainly corresponds to the dehydrogenation of ZrH_2 are shown in Fig. 16. Details are discussed later.

4. Discussion

During the reactive mechanical grinding in this work, the particles ground under hydrogen-containing atmospheres transform into hydride phases within 5 min from the beginning of grinding. Therefore, we can recognize that further grinding substantially restarts from such stabilized phases. Then they are continuously transformed into a-$Zr_{1-\delta}NiH_x$ as a metastable state or into a hydride of Zr as a stable state.

Regarding the changes in particle sizes, the diameters estimated from the SEM images in Figs. 7–10 are summarized in Fig. 17. It can be deduced from comparison of Figs. 3–6 with Fig. 17 that the reductions of particle sizes effectively progress as long as only ZrNiH and/or $ZrNiH_3$ exist in each particle. However, even the particles with reduced sizes in the earlier stage of the grinding become coarser with the growth of the amorphous phase.

In addition to the reduction of particle sizes, the mechanical grinding under hydrogen-containing atmospheres possesses two substantial advantages. The first is that ZrH_2, which was formed from the initial compound ZrNi, could be formed even at room temperature. Without grinding, the decomposition to form ZrH_2 will not progress only by hydriding reaction around room temperature. In this work, ZrH_2 was formed directly from a-$Zr_{1-\delta}NiH_x$. Therefore, because of the grinding effects, it is considered that elemental Zr at the surface of each particle easily changes its binding state to form the hydride phase. Some amount of ZrH_2, which was formed at the surface, seems to penetrate into the host particles with progression of grinding. Therefore, if the formation of ZrH_2 starts to be suppressed with the decrease in active elemental Zr near the surface, the amount of ZrH_2 at the surface of each particle will decrease because of the penetration into the host particles. This agrees reasonably with the experimental results (Figs. 4 and 5) that the intensities of peaks corresponding to ZrH_2 in the X-ray diffraction profiles show a maximum around 20 h from the beginning of grinding.

The second advantage is related to the peculiar crystallization and dehydrogenation properties of the particles ground under 1.0 MPa of pure hydrogen for 80 h, as described in Section 3.4. These particles consist of the phases such as ZrH_2, $ZrNiH_3$ and a-$Zr_{1-\delta}NiH_x$, as shown in Figs. 6(d) and 16(a). We assume that these properties originate from the existence of the $ZrNiH_3$ phase in each particle because of the high chemical potential of hydrogen. This hydride phase cannot exist in the particles ground for 80 h under lower partial pressures.

During the heating process under a pure argon atmosphere, the particles start to dissociate hydrogen

atoms which formed the $ZrNiH_3$ phase and which were trapped by unstable sites in a-$Zr_{1-\delta}NiH_x$. At 693 K, as is evident from Fig. 16(b), the particles consist of phases such as ZrH_2, dehydrided crystalline ZrNi and a-$Zr_{1-\delta}NiH_x$ just before the crystallization.

With further heating around 750 K, the a-$Zr_{1-\delta}NiH_x$ can preferentially transform into new crystalline ZrNi, which seems to be a stable structure at this temperature, because the dehydrided crystalline ZrNi is already dispersed in each particle and forms nucleation sites for crystallization. During this crystallization reaction, elemental Zr in ZrH_2 is consumed to form new crystalline ZrNi from the a-$Zr_{1-\delta}NiH_x$ in which the atomic ratio of elemental Zr is less than that of Ni. This consumption of elemental Zr inevitably promotes the dehydrogenation of ZrH_2 as shown in Fig. 16(c). We believe that the exothermic peak corresponding to crystallization of a-$Zr_{1-\delta}NiH_x$ is rather broad because of the gradual crystallization reaction. Therefore, the exothermic peak is most likely hidden by the large endothermic peak in Fig. 15 ($T_d = 746$ K), which corresponds to both the dehydrogenation of ZrH_2 and dissociation of the hydrogen trapped by the a-$Zr_{1-\delta}NiH_x$.

We conclude that the preferential crystallization induces the low-temperature dehydrogenation of ZrH_2. Since the other particles ground under lower partial pressures of hydrogen do not have ZrNi phase as nucleation sites for crystallization (shown in Figs. 5(f) and 14(a) for the particles ground under 0.3 MPa of hydrogen), a-$Zr_{1-\delta}NiH_x$ tentatively transforms into the metastable Zr_7Ni_{10} at the same temperature, as shown in Fig. 14(b). In this case dehydrogenation of ZrH_2 can proceed only at higher temperatures around 810 K by the solid–solid reaction between ZrH_2 and Zr_7Ni_{10} (shown in Fig. 14(c)).

Because of the advantages of the reactive mechanical grinding in this work, this grinding technique is now being applied to the design of materials for hydrogen storage which have microscopic interfaces of amorphous and crystalline phase, or for hard magnets with anisotropic nanoscale grains which are expected to be formed by utilizing successive hydrogenation, amorphization and dehydrogenation–crystallization reactions. Moreover, TEM observations of synthesized particles are in progress to clarify the microstructures in the composite phase. According to the preliminary results, composite particles of amorphous-like and crystalline phases were observable. Further investigations concerned with the nanoscale structures of these phases should be carried out in detail.

5. Conclusions

In the reactive mechanical grinding of ZrNi under various partial pressures of hydrogen, we obtained the following results:

(1) At the beginning of grinding, hydride phases are formed to lower the free energy of the compound, and particle sizes are effectively reduced.

(2) With progression of the grinding, an amorphous phase starts to grow.

(3) Finally, depending on the partial pressure of hydrogen, composite particles of amorphous hydride (a-$Zr_{1-\delta}NiH_x$) phase and crystalline hydride ($ZrNiH_3$ and/or ZrH_2) phases are synthesized.

(4) In the synthesized particles, the decomposition reaction to form ZrH_2 was strongly enhanced.

(5) The coexistence of a-$Zr_{1-\delta}NiH_x$ and crystalline $ZrNi(H_3)$ in each particle leads to preferential crystallization into a ZrNi phase and also to low-temperature dehydrogenation of ZrH_2.

Acknowledgements

We express our gratitude to Professor K. Aoki of the Institute for Materials Research, Tohoku University, for valuable discussions. We also acknowledge Professor Y. Kitano of the Faculty of Science, Hiroshima University, for TEM observations.

References

[1] A.Y. Yermakov, Y.Y. Yurchikov and V.A. Barinov, *Phys. Met. Metall., 52* (1981) 50.
[2] R.B. Schwarz, R.R. Petrich and C.K. Saw, *J. Non-Cryst. Solids, 76* (1985) 281.
[3] R.B. Schwarz and C.C. Koch, *Appl. Phys. Lett., 49* (1986) 146.
[4] Y.S. Cho and C.C. Koch, *J. Alloys Comp., 194* (1993) 287.
[5] K. Suzuki and T. Fukunaga, *J. Alloys Comp., 194* (1993) 303.
[6] M.S. El-Eskandarany, K. Aoki and K. Suzuki, *Appl. Phys. Lett., 60* (1992) 1562.
[7] K. Aoki, A. Memezawa and T. Masumoto, *Appl. Phys. Lett., 61* (1992) 1037.
[8] K. Aoki, A. Memezawa and T. Masumoto, *J. Mater. Res., 8* (1993) 307.
[9] A. Memezawa, K. Aoki and T. Masumoto, *Scr. Metall., 28* (1993) 361.
[10] J. Hunt, I. Soletta, L. Battezzati, N. Cowlam and G. Cocco, *J. Alloys Comp., 194* (1993) 311.
[11] D.G. Westlake, H. Shaked, P.R. Mason, B.R. MaCart, M.H. Mueller, T. Masumoto and M. Amano, *J. Less-Common Met., 88* (1982) 17.
[12] E. Batalla, J.O. Strom-Olsen, Z. Altounian, D. Boothroyd and R. Harris, *J. Mater. Res., 1* (1986) 765.
[13] J.H. Harris, W.A. Curtin and L. Schultz, *J. Mater. Res., 3* (1988) 872.
[14] T. Araki, T. Abe and K. Tanaka, *Mater. Trans. Jpn. Inst. Met., 30* (1989) 748.
[15] T.H. Jang and J.Y. Lee, *J. Non-Cryst. Solids, 116* (1990) 73.
[16] K. Aoki and T. Masumoto, *J. Jpn. Inst. Met., 49* (1985) 89.